Bull. Natl. Mus. Nat. Sci., Ser. C, 49, pp. 29–43, December 20, 2023

DOI: 10.50826/bnmnsgeopaleo.49.0_29

Additional specimens of index conodonts from the Lower Triassic Lang Son and Bac Thuy formations, Lang Son Province, northeastern Vietnam

Takumi Maekawa[1, *], Toshifumi Komatsu[2], Phong Nguyen Duc[3], Tien Dinh Cong[3] and Huyen Dang Tran[3]

[1]Osaka Museum of Natural History, 1–23 Nagai Park, Higashi-shumiyoshi-ku, Osaka 546–0034, Japan
[2]Faculty of Advanced Science and Technology, Kumamoto University, 2–39–1 Kurokami, Chuo-ku, Kumamoto 860–8555, Japan
[3]Department of Paleontology and Stratigraphy, Vietnam Institute of Geosciences and Mineral Resources (VIGMR), Hanoi, Vietnam
*Author for correspondence: tmaekawa@omnh.jp

Abstract Newly identified specimens of Early Triassic conodont species were found in the Lang Son area, northern Vietnam. *Eurygnathodus costatus* Staesche, 1964 was found in the Smithian (lower Olenekian) part of the Lang Son Formation in Route A of Ky Cung River area. *Icriospathodus zaksi* (Buryi) and *Novispathodus* sp. C were found in the uppermost Smithian part of the Bac Thuy Formation in Ban Ru area. These species update the regional biostratigraphical successions of the Lang Son and Bac Thuy formations. In addition, the Lang Son and Bac Thuy formations will be good reference sections to study the presumed evolutionary trends of *Eu. costatus* and *Ic. zaksi*, respectively.

Key words: *Eurygnathodus*, *Icrispathodus*, Induan, *Novispathodus*, Olenekian

Introduction

During the Early Triassic, northeastern Vietnam was in the southern part of the South China Block and the An Chau Basin, which is the southern part of the large Nanpanjian Basin (Fig. 1A; Galfetti *et al.*, 2008; Komatsu *et al.*, 2014, 2016; Shigeta *et al.*, 2014). The Early Triassic An Chau Basin is filled mainly with marine deposits of the Lower Triassic Lang Son and Bac Thuy formations and the Middle Triassic Khon Lang Formation (Fig. 1B; Dang, 2006; Shigeta *et al.*, 2014). The Lang Son Formation consists mainly of siliciclastic rocks such as mudstone and sandstone, and is conformably overlain or interfingered by the Bac Thuy Formation, which consists mainly of mudstone and carbonate rocks such as bioclastic limestone, bedded limestone, and limestone breccia (Fig. 2; Komatsu *et al.*, 2014; Shigeta *et al.*, 2014). The two formations are partly in a relationship of contemporaneous heterotopic facies and are unconformably overlain by volcanic rocks of the Khon Lang Formation (Figs. 1B, 2; Dang, 2006; Komatsu *et al.*, 2014).

The Induan to Smithian (early Olenekian) age of the Lang Son Formation has been inferred from bivalve fossils (Dang, 2006; Komatsu and Dang, 2007). Recently, Maekawa *et al.* (2015) reported an early Smithian conodont association such as *Eurygnathodus costatus* Staesche, 1964, *Eu. hamadai* (Koike, 1982), *Neospathodus cristagalli* (Huckriede, 1958), and *Ns. pakistanensis* Sweet, 1970 from the upper part of the Lang Son Formation in the Ky Cung River area, Lang Son Province. Thus, in that area the Induan–Olenekian boundary (IOB) is probably located in the upper part of the formation. Takahashi *et al.* (2022) newly reported radiolarian fossils from the same locality of Maekawa *et al.* (2015).

Carbonate and siliciclastic rocks of the Bac Thuy Formation contain abundant marine mega- and micro-fossils such as ammonoids, gastropods, bivalves, conodonts, ostracods, and radiolarians (Vu Khuc, 1984, 1991; Bui, 1989; Dang, 2006; Komatsu *et al.*, 2013, 2014, 2016; Shigeta *et al.*, 2014; Maekawa *et al.*, 2016; Takahashi *et al.*, 2017). According to Shigeta *et al.* (2014), the age of the Bac Thuy Formation is middle Smithian to early Spathian (late Olenekian) on the basis of age-diag-

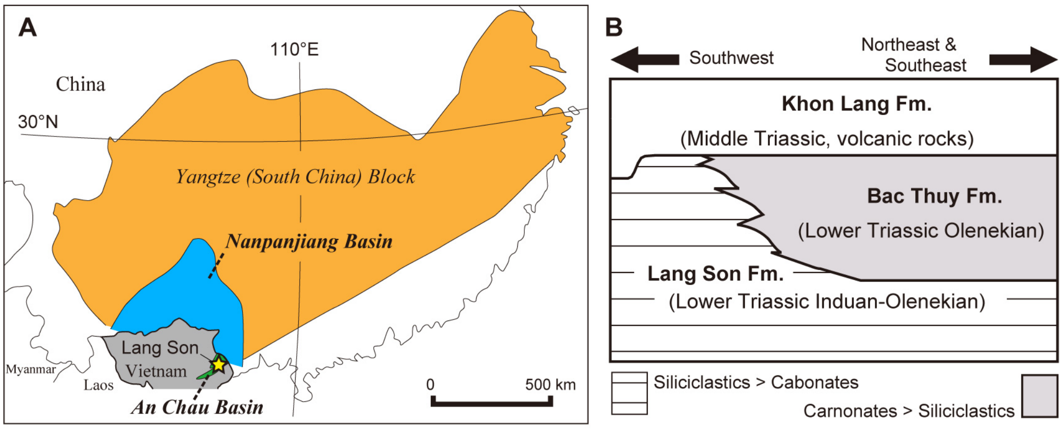

Fig. 1. Index map and stratigraphic subdivision. A. Geographic map of East Asia with distribution of the South China block, Nanpanjian Basin and An Chau Basin, modified from Komatsu *et al.* (2014). B. Stratigraphic subdivision of An Chau Basin, modified from Shigeta *et al.* (2014).

nostic ammonoids and conodonts; e.g., *Owenites koeneni* Hyatt and Smith, 1905, *Xenoceltites variocostatus* Brayard and Bucher, 2008, *Novispathodus* ex gr. *waageni* (Sweet, 1970), and *Nv*. ex gr. *pingdingshanensis* (Zhao and Orchard in Zhao *et al.*, 2007). Maekawa *et al.* (2016) reported Dienerian (late Induan) conodonts from basal limestone beds of the Bac Thuy Formation in Locality BR00 of the Ban Ru area. The geological age of the Bac Thuy Formation is thus the late Induan to late Olenekian, and the formation contains the IOB and the Smithian–Spathian boundary (SSB). The SSB is defined by the first occurrence of the basal Spathian ammonoid *Tirolites* cf. *cassianus* (Quenstedt, 1849) (Shigeta *et al.*, 2014; Komatsu *et al.*, 2016). In addition, latest Smithian to early Spathian conodont taxa such as *Nv*. ex gr. *pingdingshanensis*, *Nv. brevissimus* (Orchard, 1995), and *Icriospathodus collinsoni* (Solien, 1979) have been reported from the Bac Thuy Formation (Shigeta *et al.*, 2014; Komatsu *et al.*, 2016; Maekawa *et al.*, 2021).

In this study, we describe one conodont species from the Lang Son Formation and two from the Bac Thuy Formation. The occurrences and descriptions of these three species updated the regional biostratigraphy and systematic paleontology of these Olenekian conodonts.

Geological Setting

Geology and stratigraphy of the Lang Son and Bac Thuy formations which were distributed in Lang Son City and Chi Lang District have been studied and reported by Dang (2006), Komatsu *et al.* (2014, 2016), Shigeta *et al.* (2014), Takahashi *et al.* (2017, 2022). According to the reports, there are five studied areas (Bac Thuy, Ban Ru, Ky Cung River, Na Trang, Pac Khonh) in Lang Son City and Chi Lang District. In this study, we additionally studied Route A in Ky Cung River area, and BR01 in Ban Ru area, but we generally follow geological and stratigraphical data of mensioned prior reports. Columner sections of each areas concluded in Fig. 2.

The Lang Son Formation in Lang Son City

We studied the Lang Son Formation distributed along a branch of the Ky Cung River located in the central part of Lang Son City (Fig. 1C, D). In the study section (Route A of Fig. 3A, B), the upper part of the Lang Son Formation (= Member “3” in Dang, 2006), consists of alternations of fine-grained sandstone and mudstone occasionally intercalating with thin limestone and marl bed, crop out. In Locality 01, several thin bioclastic and micritic limestone beds (1–5 cm thick) contain some microfossils such as conodonts, small bivalves, fish teeth, and radiolarians (Maekawa *et al.*, 2015; Takahashi *et al.*, 2022). Maekawa *et al.* (2015) reported Smithian conodont association from Loc. 01-01 (= 01-C of Takahashi *et al.*, 2022) which is a bioclastic limestone bed (Fig. 3C). A limestone sample (Loc. 01-00 = 01-B of Takahashi *et al.*, 2022) was collected from 10 cm below Loc. 01-01 for conodont analysis in this study.

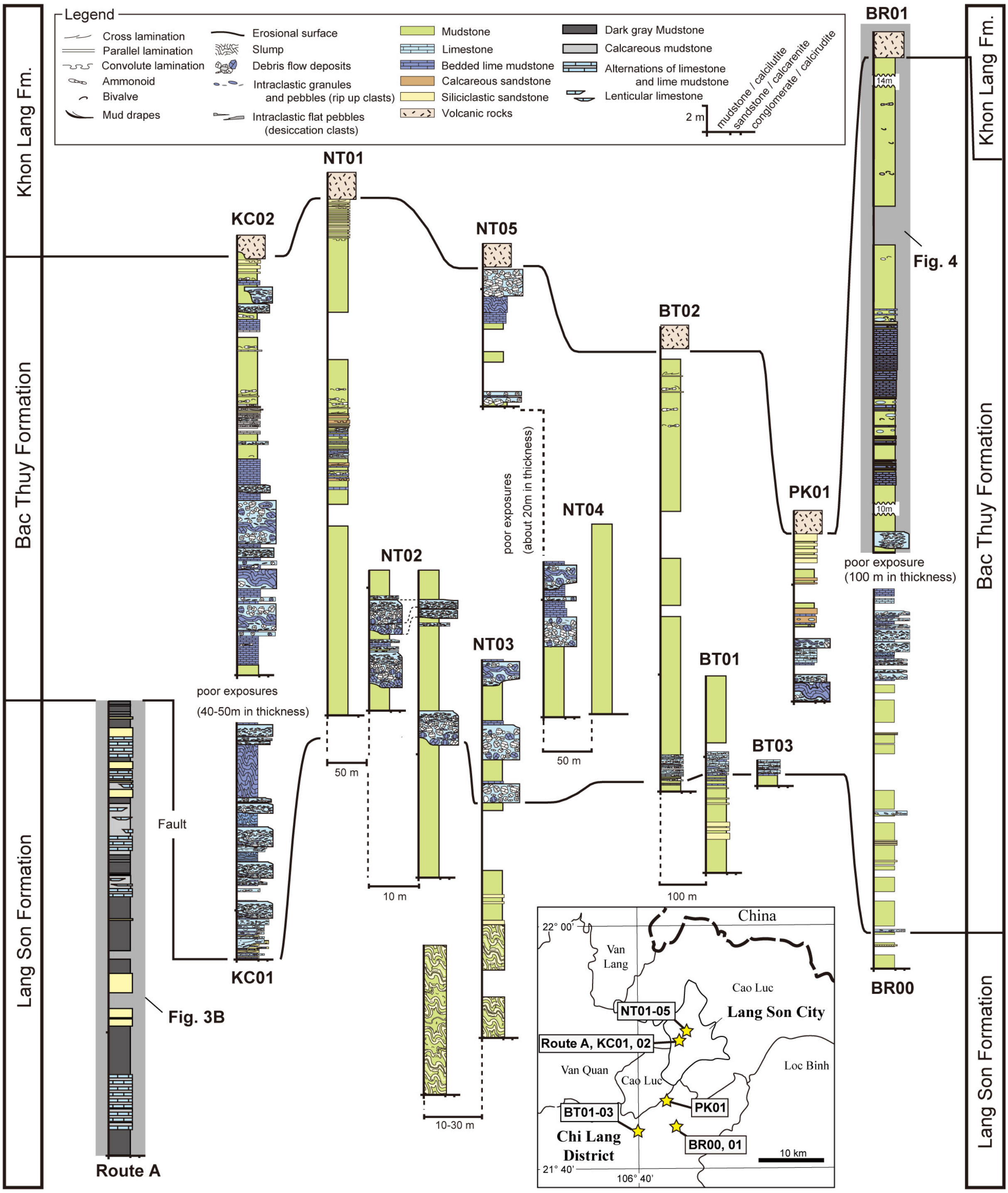

Fig. 2. Map with studied areas of Lang Son Province, northeastern Vietnam and columnar sections of each areas, modified from Shigeta *et al.* (2014) and Takahashi *et al.* (2022).

The Bac Thuy Formation

Ban Ru area

The two studied sections (BR00 and BR01) are located in the Ban Ru area, Chi Lang District (Fig. 2). In this area, the total thickness of the Bac Thuy Formation exceeds 185 m (Dang, 2006). According to Shigeta *et al.* (2014) and Komatsu *et al.* (2016), the Bac Thuy Formation is generally divided into lower, middle, and upper parts. The lower part of the formation can be observed in section BR00, and the middle and upper parts in section BR01 (Shigeta *et al.*, 2014; Maekawa *et al.* 2016): the lower part (over 130 m thick)-composed mainly of mudstone, limestone breccia and bedded limestone; the middle part (13 m thick)-consists predominately of dark gray organic-rich thin bedded limestone and mudstone containing dark gray calcareous nodules that commonly yield ostracods and bivalves; the upper

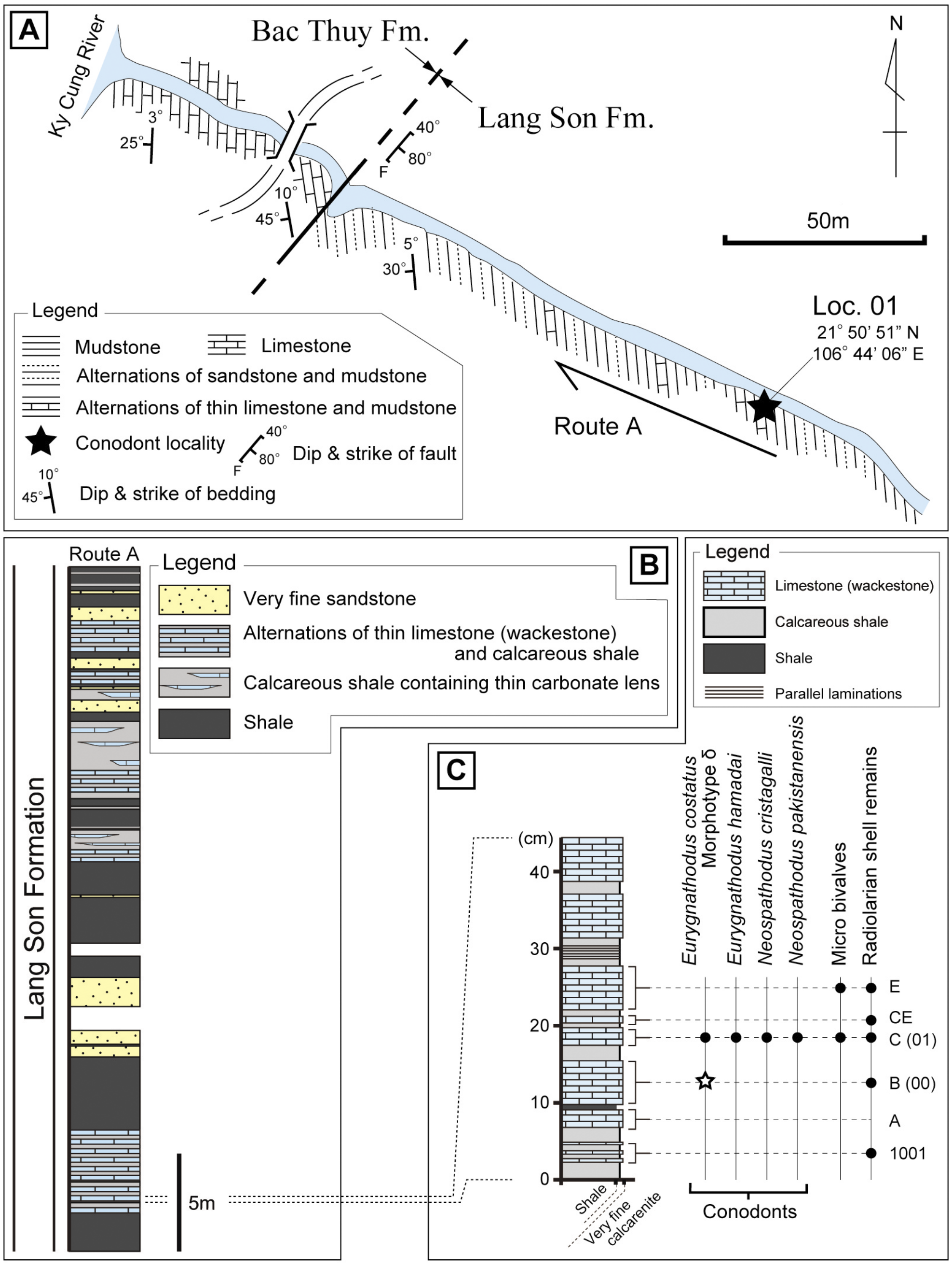

Fig. 3. Route map and columnar sections of Ky Cung River area. A. Route map with locality 01, modified from Maekawa *et al.* (2015). B. Columnar section of Route A. C. Enlarged columnar section of locality 01 with distributions of conodont taxa and other microfossils.

part (30 m thick)-dominated by thick greenish gray mudstone. Conodont elements were newly recovered from a bedded lime mudstone (BR01-02) in BR01 (Fig. 4).

Material and Method

We collected limestone samples from Locality 01-00 of the Lang Son Formation, Lang Son City and BR01-02 of the Bac Thuy Formation, Chi Lang District. Each 1 kg sample was crushed to fragments about 1–3 cm across and immersed in an 8–10% solution of acetic acid for 2 days to dissolve carbonates. Subsequently, the residue was collected using 1.0 mm and 0.177 mm meshes. This procedure was repeated until all carbonate had been completely dissolved.

Conodont elements and some microfossils were picked from the residues using a light microscope PLYMPUS SZX7 (Olympus Co., Ltd., Tokyo). Conodont samples were captured images using scanning electron microscope JEOL JSM-6360LV

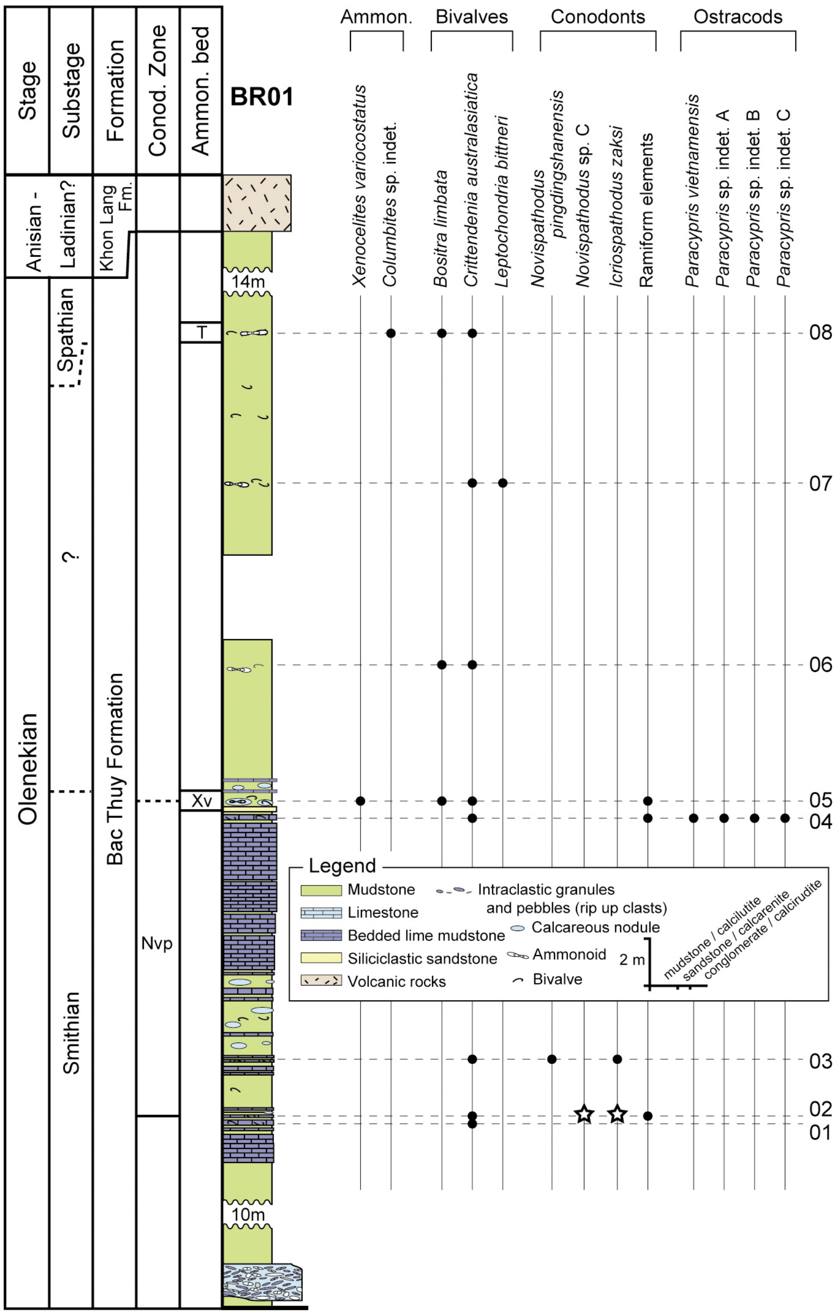

Fig. 4. Columnar section of the Bac Thuy Formation in BR01, Ban Ru area with distributions of ammonoid, bivalve, conodont and ostracoda taxa, modified from Shigeta *et al.* (2014). Abbreviations: Conod., Conodont; Ammon., Ammonoid; Nvp, *Novispathodus pingdingshanensis* Zone; Xv, *Xenoceltites variocostatus* beds; T, *Tirolites* sp. nov. beds.

(Jeol Ltd., Tokyo).

Systematic Paleontology

by T. Maekawa

Locational notation of conodont elements has largely been modified by intensive analysis of multielement reconstruction of conodont apparatuses (e.g., Purnell *et al.*, 2000). All specimens described herein are discrete P_1 elements; hence, the orientation terms proposed by Sweet (1988), Purnell *et al.* (2000) and Orchard (2005) has also been adopted. Measurements are shown in Table 1.

Described conodont specimens are reposited in the Micropaleontology Collection (MPC) of the National Museum of Nature and Science (NMNS), Tsukuba. All specimens show dark gray color which probably corresponds to CAI 3–4 of Epstein *et al.* (1977).

Table 1. Measurements of described conodont specimens in this paper. "+" shows incomplete measurements on broken specimens.

Figure no.	Species	Specimen no.	Element				Basal cavity			Denticle no.	Remarks
			Length (mm)	Height (mm)	Width (mm)	L/H	Length (mm)	Width (mm)	Form		
5A	*Eurygnathodus costatus*	MPC-42850	1.01	0.23	0.53	4.39	0.73	0.46	—	10	Morphotype δ
5B	*Novispathodus* sp. C	MPC-42851	0.43	0.31	0.05	1.40	0.2 +	0.21	Round	10	Broken basal cavity
5C	*Icriospathodus zaksi*	MPC-42852	0.42	0.29	0.09	1.40	0.22	0.16	Drop	7	
5D	*Icriospathodus zaksi*	MPC-42853	0.42 +	0.29 +	0.09	—	—	0.18 +	—	6 +	Broken element
5E	*Icriospathodus zaksi*	MPC-42854	0.46	0.30	0.16	1.50	0.19	0.26	Asymmetrical oval	8	
5F	*Icriospathodus zaksi*	MPC-42855	0.53	0.29	0.11	1.80	0.22	0.29	Elliptical	9	
5G	*Icriospathodus zaksi*	MPC-42856	0.44	0.27 +	0.12	1.60	0.19	0.23	Oval	9	Broken element

Class Conodonta Eichenberg, 1930
Order Ozarkodina Dzik, 1976
Superfamily Gondolelloidea (Lindström, 1970)
Family Gondolellidae Lindström, 1970
Subfamily Novispathodontinae Orchard, 2005
Genus ***Novispathodus*** Orchard, 2005

Type species: *Neospathodus abruptus* Orchard, 1995

Novispathodus sp. C

Fig. 5B

Novispathodus sp. nov. C Goudemand and Orchard in Goudemand *et al.*, 2012, p. 1032, fig. 2O; Maekawa in Maekawa *et al.*, 2018, p. 43, figs. 24.1–24.3.

Material examined: One specimen, MPC-42851, from BR01-02.

Distributions and age: The species has been reported from the *Novispathodus pingdingshanensis* Zone of South China (Goudemand *et al.*, 2012) and Southwest Japan (Maekawa *et al.*, 2018). Thus, the species generally indicates the latest Smithian age.

Description: Segminate element 0.43 mm in length; 0.31 mm in height; length to height ratio 1.4. Strongly fused denticles with triangular tip, 10 in number which contain smallest terminal denticle, progressively reclined posteriorly. Basal margin upturned in anterior and up-arched beneath basal cavity. Basal cavity, rounded outline, although partly broken, occupies over half of element length, slightly concave. A groove runs from the basal pit to anterior end.

Remarks: *Novispathodus* sp. C, originally reported from South China by Goudemand *et al.* (2012), is characterized by the large rounded basal cavity and gradually reclined denticulation with small terminal denticle. Those features are similar to the Vietnamese specimen described herein.

Subfamily uncertain
Genus ***Eurygnathodus*** Staesche, 1964

Type species: *Eurygnathodus costatus* Staesche, 1964.

Eurygnathodus costatus Staesche, 1964

Fig. 5A

Eurygnathodus costatus Staesche, 1964, p. 269, pl. 28, figs. 1–6; Budurov and Pantic, 1973, p. 51, pl. 1, figs. 1–15; Igo, 2009, p. 183, figs. 152.23, 152.24; Orchard, 2010, figs. 5.9, 5.10; Maekawa and Igo, 2014, p. 220, 222, figs. 161.4–161.6; Chen *et al.*, 2015, fig. 8.4; Maekawa in Maekawa *et al.*, 2015, p. 316, 317, fig. 5.2; Chen *et al.*, 2016, figs. 10.7–10.10, 11.3. 11.6, 11.7; Maekawa in Maekawa *et al.*, 2018, p. 45, figs. 25–27; Li *et al.*, 2022, fig. 5.1; Chen *et al.*, 2022, figs. 10.7, 10.11–10.18.

Eurygnathodus ex gr. *costatus* Staesche. Lyu *et al.*, 2020, p. 10, figs. 7–9.

Platyvillosus costatus (Staesche), Goel, 1977, p. 1098, pl. 2, figs. 15–21; Wang and Cao, 1981, p. 371, pl. 2, figs. 1–4, 28, 29, 30, 33; Koike, 1982, p. 44, pl. 5, figs. 1–9; Tian *et al.*, 1983, p. 391, pl. 81, fig. 2; Matsuda, 1984, p. 128, pl. 6, figs. 6–10; Duan, 1987, pl. 3, fig. 4; Koike, 1988, pl. 1, figs. 1–57, pl. 2, figs. 1–37; Bui, 1989, p. 411, pl. 31, figs. 7–9; Beyers and Orchard, 1991, pl. 5, fig. 10; Cao and Wang, 1993, pl. 56, fig. 16; Wang and Zhong, 1994, p. 404, pl.1, figs. 15, 23.

Platyvillosus paracostatus, Wang and Cao, 1981, p. 371, pl. 2, figs. 9, 10.

Eurygnathodus hamadai (Koike, 1982), Chen *et al.*, 2016, fig. 11.1; Chen *et al.*, 2022, figs. 10.20, 10.22.

Eurygnathodus sp. A. Lyu *et al.*, 2020, fig. 12.11.

Eurygnathodus sp. B. Lyu *et al.*, 2020, fig. 12.12; Chen *et al.*, 2022, fig. 10.1.

Eurygnathodus sp. C. Lyu *et al.*, 2020, fig. 12.31.

Eurygnathodus sp. D. Lyu *et al.*, 2020, figs. 12.20–12.23; Chen *et al.*, 2022, figs. 10.2–10.6.

Eurygnathodus sp. E. Lyu *et al.*, 2020, fig. 12.16.

Eurygnathodus sp. F. Lyu *et al.*, 2020, figs. 12.17, 12.18; Chen *et al.*, 2022, fig. 10.8.

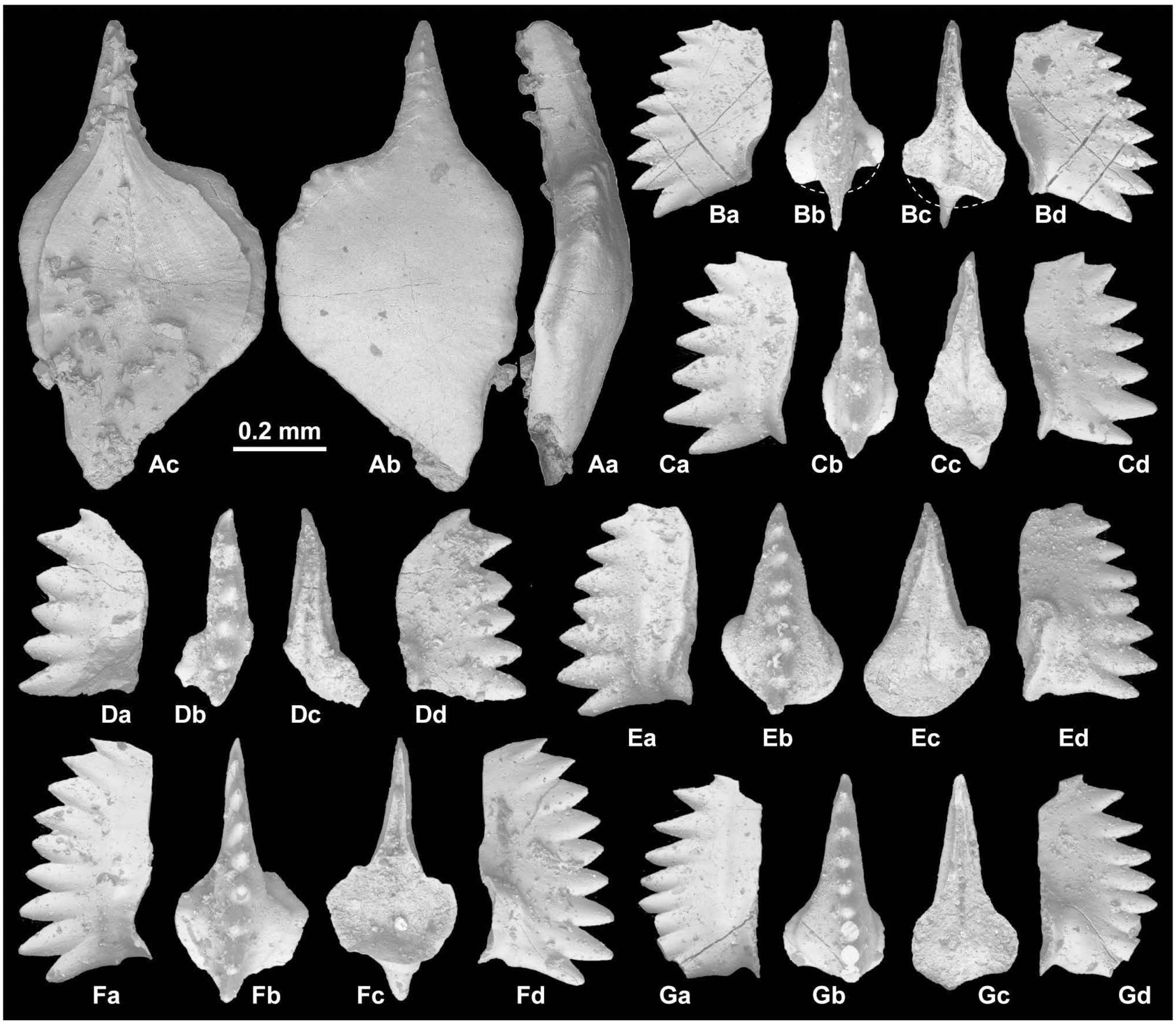

Fig. 5. SEM images of P_1 elements of conodonts from the Lang Son and Bac Thuy formations. A. *Eurygnathodus costatus* Staesche, 1964, MPC-42850. B. *Novispathodus* sp. C, MPC-42851. C–G. *Icriospathodus zaksi* (Buryi, 1979); 3, MPC-42852; 4, MPC-42853; 5, MPC-42854; 6, MPC-42855; 7, MPC-42856. 1 from Loc. 01-00; 2–7 from BR01-02. For 1–7: a, d, lateral views; b, upper view; c, lower view.

Eurygnathodus sp. G. Lyu *et al.*, 2020, fig. 12.19.

Material examined: One specimen, MPC-42850, from Loc. 01-00.

Distributions and age: This species has been reported from South Tirol (Staesche, 1964), Spiti, India (Goel, 1977; Krystyn *et al.*, 2007, Orchard and Krystyn, 2007; Orchard, 2010), South China (Wang and Cao, 1981; Wang and Zhong, 1994; Zhao *et al.*, 2007; Chen *et al.*, 2015, 2022; Lyu *et al.*, 2020), Kashmir, India (Matsuda, 1984), Southwest Japan (Koike, 1988; Maekawa *et al.*, 2018), northeastern Vietnam (Bui, 1989; Maekawa and Igo, 2014; Maekawa *et al.*, 2015), British Columbia, Canada (Beyers and Orchard, 1991), South Primorye, Russia (Shigeta *et al.*, 2009), Slovenia (Chen *et al.*, 2016), and northwestern China (Li *et al.*, 2022). The stratigraphic distribution of this species well correlates to the *Flemingites–Euflemingites* beds of some of the mentioned localities (Orchard and Krystyn, 2007; Shigeta *et al.*, 2009, 2014). According to Krystyn *et al.* (2017) and Lyu *et al.* (2020), the first occurrence (FO) of this species is situated below the FOs of *Novispathodus waageni* or *Novispathodus eowaageni* (Zhao and Orchard in Zhao *et al.*, 2007) which are indicators of the IOB in conodont biostratigraphy. Thus, *Eu*. *costatus* ranges from the uppermost Dienerian to middle Smithian.

Description: One segminiplanate element 1.01 mm in length; 0.53 mm in width; 0.23 mm in height. In the upper view, sub-rounded platform has narrow anterior “free blade” and sub-triangular posterior margin. The “free blade” bears small denticles, 5 in number. Anterior platform margin bears node-like denticles, 6 in number. In the lateral view, the element is arched. In the lower view, the outline of the basal cavity is similar to that of the platform. A groove runs from the basal pit to anterior end of “free blade”.

Remarks: Variation of the ornamentation of *Eu. costatus* has been studied by some researchers (e.g., Matsuda, 1984; Koike, 1988; Maekawa *et al.*, 2018; Lyu *et al.*, 2020). Koike (1988) divided the species into the holotype form (Form A) and four morphotypes (α, β, γ, δ) as follows: Form A-transverse ridges covers the entire platform surface; Morphotype α-characterized by narrow ridges which are restricted in the center of the element; Morphotype β-has fine ridges and central nodose denticles; Morphotype γ-has nodose denticles which show regular and/or chaotic arrangements; Morphotype δ-has faint ridges which cover all or a part of the platform surface. On the other hand, Lyu *et al.* (2020) splitted some morphotypes from typical form of *Eu. costatus* and recognized seven species of the genus *Eurygnathodus*. In this study, we follow Koike (1988)’s recognition. The small denticles of the Vietnamese specimen are probably traces of diminished ridges. Thus, according to the definition of Koike (1988), the described specimen belongs to Morphotype δ of *Eu. costatus*.

The platform outline of Morphotype δ generally shows a bilaterally asymmetrical form, and the feature is common in the P_1 element of *Eu. hamadai* which lacks ornamentations on the platform (Koike, 1982; Maekawa *et al.*, 2018; Lyu *et al.*, 2020). In addition, the latter species occurs later than the former (Orchard and Krystyn, 2007; Lyu *et al.*, 2020). Thus, *Eu. costatus* Morphotype δ is a probable ancestor of *Eu. hamadai*. These results well support an evolutional hypothesis of Maekawa *et al.* (2015) and Lyu *et al.* (2020), but it is still unknown why the ornamentation became diminished.

Genus ***Icriospathodus*** Krahl, Kauffmann, Kozur, Richter, Foerster and Heinritzi, 1983

Type species: *Neospathodus collinsoni* Solien, 1979.

Icriospathodus zaksi (Buryi, 1979)

Fig. 5C–G

Neospathodus zaksi Buryi, 1979, p. 60, pl. 18, fig. 3a, b.
Neospathodus triangularis (Bender, 1970). Perri and Andraghetti, 1987, p. 311, pl. 33, figs. 1–4.
Icriospathodus? *zaksi* (Buryi). Orchard, 2007, p. 105, fig. 2; Maekawa and Igo, 2014, p. 267, 268, figs. 192.14–192.29; Komatsu *et al.*, 2016, figs. 5.2, 5.3.
Neospathodus robustus Koike, 1982. Chen and Kolar-Jurkovšek in Chen *et al.*, 2016, fig. 8.8.
Neospathodus planus Chen and Kolar-Jurkovšek in Chen *et al.*, 2016, fig. 8.10.
Icriospathodus zaksi (Buryi). Maekawa in Maekawa *et al.*, 2018, p. 52, figs. 29.20–29.26; Chen *et al.*, 2019, figs. 6.4, 7.9, 7.10.
Icriospathodus crassatus (Orchard, 1995). Chen *et al.*, 2019, figs. 3.13, 5.8; Chen *et al.*, 2021, figs. 3.11, 6.10.

Material examined: Five specimens, MPC-42852–42856, from BR01-02.

Distributions and age: This species occurs from South Primorye, Russia (upper part of the *Anasibirites nevolini* Zone and lower part of the *Tirolites cassianus* Zone, Buryi, 1979), the Werfen Formation, southern Alps, Italy (Perri and Andraghetti,

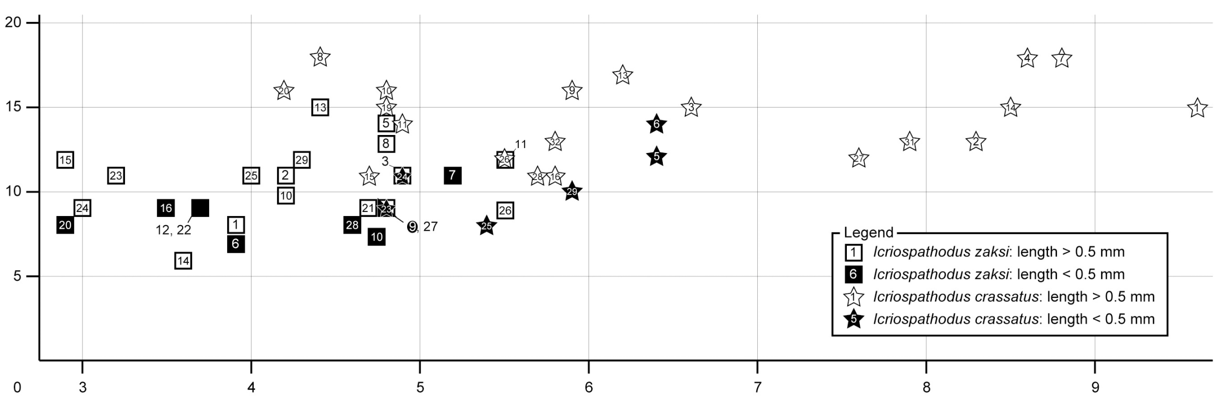

Fig. 6. Scatter diagram showing the relationship between denticle number and length/width ratio in *Icriospathodus crassatus* and *Ic. zaksi*. The number inside squares and star marks corresponds to “Number” in Appendix (Iz1–29, Ic1–32). Broken specimens (Iz4, Iz17, Iz19, Ic12, Ic17, Ic18, Ic21, Ic22, Ic30) were unshown.

1987), the Bac Thuy Formation, northeastern Vietnam (the *Novispathodus* ex gr. *pingdingshanensis* Zone in the *Xenoceltites variocostatus* beds, Shigeta *et al.*, 2014; Komatsu *et al.*, 2016; this study), Slovenia (Chen *et al.*, 2016), the Taho Formation, Southwest Japan (the *Novispathodus brevissimus* Zone, Maekawa *et al.*, 2018), and Oman (Chen *et al.*, 2019; Chen *et al.*, 2021). According to those reports, the species ranges from the latest Smithian to early Spathian.

Description: Five robust rectangular segminate P_1 elements 0.42–0.53 mm in length; 0.27–0.30 mm in height; 0.09–0.16 mm in width; length to height ratio 1.4–1.8. Robust and strongly fused denticles with sub-triangular tip, 7 to 9 in number, erect or radial fashion. Upper edge gradually increases height to posterior cusp which is situated in front of the terminal denticle. Basal margin is straight or upturned in anterior and up-arched beneath basal cavity. Posterior margin abrupt or slightly reclined posteriorly. Laterally expanded basal cup developed on oval, drop-like or elliptical basal cavity. One specimen (Fig. 5E, MPC-42854) has an asymmetrical oval basal cavity. Groove runs from basal pit to anterior end.

Remarks: The described specimens are smaller and/or more slender than the specimens from the Ky Cung and Na Trang areas (see Appendix; 0.49–0.65 mm in length, 0.14–0.21 mm in width; Shigeta *et al.*, 2014), but the robust unit with erect and robust denticles of the Ban Ru specimens are similar to specimens from those two areas. The difference in element size of specimens from Ban Ru and the other areas simply suggests that the Ban Ru specimens are stratigraphically older than the others. In addition, the sub-triangular tip of the fused denticulation and small element size of the Ban Ru specimens imply that the species evolved from a species of the genus *Novispathodus*, which dominates the latest Smithian ammonoid *Xenoceltites variocostatus* beds of Vietnam and South China (Goudemand *et al.*, 2012; Shigeta *et al.*, 2014). Thus, the Ban Ru specimens probably fill the philogenetic gap of these two genera.

According to the Vietnamese data (Maekawa and Igo, 2014; this study), *Ic. zaksi* is a probable rootstock of the genus because of its earliest occurrence, and some common features of the genus (robust unit and denticles, and form variations of the basal cavity) are already observed in the species. In addition, the typical form of the species is characterized by small denticle number (7 to 12), robust unit, developed basal cup, and rounded, subtriangular, rectangular or asymmetrical oval basal cavity. On the other hand, a characteristic form of the species, the P_1 element with denticles on the basal cup, appeared later than the typical form (Shigeta *et al.*, 2014; this study). On the other hand, in an Omani section, the FO of *Ic. crassatus* is slightly lower than that of *Ic. zaksi*, and specimens that bear denticles on the basal cup appeared with typical forms (Chen *et al.*, 2021). Thus, additional information from other localities is needed to decide the evolutional process of the former species and genus *Icriospathouds*.

Chen *et al.* (2021) redefined the P_1 element of *Ic. zaksi* as specimens which have denticles on the basal cup. However, the typical form of *Ic. zaksi* is well distinguished from *Ic. crassatus* by the robust unit and smaller number of denticles (Maekawa and Igo, 2014; Maekawa *et al.*, 2018), and some specimens of *Ic. collinsoni* and *Ic. crassatus* (figs. 9, 12.9, 12.10, 12.52, 13.3, 13.5–13.7 of Koike, 1992; figs. 191.2, 192.5 of Maekawa and Igo, 2014; figs. 3.14, 3.15 of Chen *et al.*, 2021) show denticles on the basal cup. Thus, the development of denticles on the basal cup is an intraspecific variation which is common in the genus. In addition, Omani specimen which has 17 denticles and a denticle on the basal cup (fig. 4.13 of Chen *et al.*, 2021) is probably classified to *Ic. crassatus*.

I also show informations of element length, width, length/width ratio, denticulation and basal cavity of three species of *Icriospathodus* from Russian, Slovenian, Italy, Omani, Vietnamese and Japanese sections (see Appendix). In addtion, a scatter diagram shows the relationship between denticle number and length/width ratio of *Ic. zaksi* (N = 26) and *Ic. crassatus* (N = 26) (Fig. 6). According to the diagram, the length/width ratio of the former species generally lower than 5.6. On the other hand, sixteen specimens of the latter species show varying lenght/width ratio from 5.7 to 9.6. The other 9 specimens of the latter species have denticles varying numer from 11 to 18, and a one specimen of the latter has 9 denticles which is shows 0.43 mm in length. Thus, above mentioned characters of *Ic.*

zaksi (robust unit and smaller number of denticles) are probably count to identiy the two species.

A specimen from Yiwagou section, northwestern China (fig. 6.16 of Li *et al.*, 2022) which has slender unit and a denticle on a side of the basal cup is clearly different from the typical from of *Ic*. *zaksi*. The specimen is a different species and probably relates to a species of genus *Triassospathodus* such as *Tr*. *qinlingensis* Li *et al.*, 2022. A Vietamese specimen (figs. 192.101–192.13 of Maekawa and Igo, 2014) which has a slender arched unit, fused 9 denticles with subtriangular tip and subrounded large basal cavity is reclassified to *Nv*. *pingdingshanensis* in this study.

Discussion

New conodont data from the Lang Son Formation: The early Smithian conodont assemblage which contains *Eurygnathodus costatus* Morphotype *δ*, *Eu*. *hamadai*, *Neospathodus cristagalli* and *Ns*. *pakistanensis* has been reported from Loc. 01-01 of the Lang Son Formation (Maekawa *et al.*, 2015). Maekawa *et al.* (2015) also assumed an evolutionary process between *Eu*. *costatus* and *Eu*. *hamadai* on the basis of data of the Lang Son Formation and that of the Taho Limestone, Southwest Japan of Koike (1988). According to the report, *Eu*. *costatus* Morphotype *δ* found slightly earlier than *Eu*. *hamadai* in southwest Japan, and the form probably indicates transitional form beween typical form of *Eu*. *costatus* and *Eu*. *hamadai*. Recently, Lyu *et al.* (2020) reported ontogeny of the former species, and proposed evolutionary process between these two species is characterized by the diminish of the ornamentaion that is similar to the assumption of Maekawa *et al.* (2015). In the present study, we reported *Eu*. *costatus* Morphotype *δ* from Loc. 01-00, Lang Son Formation, ca. 10 cm below Loc. 01-01. Although the additional data is poorly to corroborate the evolutionary senario of these two prior researches, it is following the senario. In addition, *Eu*. *costatus* Morphotype *δ* generally occurred later than the basal Smithian conodont *Novispathodus waageni* (Sweet) in Thailand (Koike, 1982) and Southwest Japan (Koike, 1988; Maekawa *et al.*, 2018). Thus, the occurrence of the morphotype *δ* probably indicates the early Smithian age.

New conodont data of the middle part of the Bac Thuy Formation in Ban Ru area: Shigeta *et al.* (2014) reported *Novispathodus pingdingshanensis* and *Icriospathodus*? *zaksi* from the middle part of the Bac Thuy Formation which distributed in KC02, NT01 and BR01 sections and established the *Nv*. *pingdingshanensis* Zone on the basis of the first occurrence of the eponimous taxa in these three area. The conodont zone was revised as *Nv*. ex gr. *pingdinshanensis* Zone by Komatsu *et al.* (2016). In the present study, we reported *Novispathouds* sp. C and *Ic*. *zaksi* from BR01-02 where is ca. 2 m below BR01-03. The former species has been reported from the *Nv*. *pingdingshanensis* Zone of South China and Southwest Japan (Gaudemand *et al.*, 2012; Maekawa *et al.*, 2018), and the range is generally limited to the latest Smithian (Gaudemand *et al.*, 2012). *Icrispathodus zaksi* probably ranges from the latest Smithian to the earliest Spathian and has been reported from the *Nv*. ex gr. *pingdingshanensis* Zone of KC02 and NT01 sections (Shigeta *et al.*, 2014; Komatsu *et al.*, 2016) and *Nv*. *pingdingshanensis* Zone of Oman (Chen *et al.*, 2019). Thus, the conodont assemblage of BR01-02 of the present study probably indicates the latest Smithian. *Novispathodus pingdingshanensis* has never been recovered from BR01-02, but in this study, we tentetively assigned the bed as a part of the *Nv*. ex gr. *pingdingshanensis* Zone.

Conclusions and Remarks

We have described one specimen of *Eurygnathodus costatus* Morphotype *δ* from Loc. 01-00 of the Lang Son Formation and one specimen of *Novispathodus* sp. C and five specimens of *Icriospathodus zaksi* from BR01-02 of the Bac Thuy Formation. It is the first report of *Novispathodus* sp. C from the Bac Thuy Formation. Based on these conodont data, in the Ban Ru area, the *Nv*. ex gr. *pingdingshanensis* Zone probably starts at BR01-02 (ca. 2 m below the level of Shigeta *et al.* (2014)). In addition, the Lang Son and Bac Thuy formations are good sections for studying processes of morphological changes of P_1 elements of *Eurygnathodus* and *Icriospathodus*, respectively. Thus, further research in these formations will be clear some problems of evolutional processes of these genera.

Acknowledgements

We thank Aaron Stallard and Sandra Purves (Stallard Scientific Editing) for English editing of the draft. We also grateful to Shun Muto (the Geological Survey of Japan) for his review with advanced comments on the draft. This study was financially supported by Grant-in-Aids for Scientific Research (KAKENHI) from the Japan Society for the Promotion of Science (16K05593, 19K04059) to T. Komatsu, and Nakatsuji Foresight Foundation Research grant and Grant-in-Aids for Young Research (KAKENHI) from the Japan Society for the promotion of Science (21K14036) to T. Maekawa.

References

Bender, H. (1970) Zhur Gliederung der Mediterrnen Trias II. Die Conodonten—chronologie der Mediterranen Trias. *Annales Geologiques des Pays Helleniques*, **19**: 465–540.

Beyers, J. N. and Orchard, M. J. (1991) Upper Permian and Triassic conodont faunas from the type area of the Cache Creek Complex, south-central British Columbia, Canada. *Geological Survey of Canada Bulletin*, **417**: 269–297.

Brayard, A. and Bucher, H. (2008) Smithian (Early Triassic) ammonoid faunas from northwestern Guangxi (South China): taxonomy and biochronology. *Fossil and Strata*, **55**: 1–179.

Budurov, K. and Pantic, S. (1973) Conodonten aus den Campiller Shichten von Brassina (Westerbien) Bulgarian Academy of Sciences. *Ministry of Heavy Industry Bulletin of the Geological Institute-Series of Paleontology*, **22**: 49–64.

Bui, D. T. (1989) Lower Triassic conodonts from North Vietnam. *Acta Palaeontologica Polonica*, **34**: 391–416.

Buryi, G. I. (1979) *Nizhnetriasovye Konodonty Yuzhnoge Primorya*, 144 pp. Institut Geologii I Geofiziki, Sibirskoye Otdeleniye, Akademiya Nauk, SSSR, Moskva. (in Russian)

Cao, Y. and Wang, Z., 1993: Triassic conodont biostratigraphy and lithofacies paleogeography. Triassic biostratigraphy section bearing conodonts. In: Wang, C. (Ed.), Conodonts of Lower Yangtze Valley-an Indexes to Biostratigraphy and Organic Metamorphic Maturity. Science Press, Beijing, pp. 103–117. (in Chinese)

Chen, A.-F., Zhang, Y., Yuan, D.-x., Wu, H.-t., Dou, J., Liu, J.-q. (2022) Upper Changhsingian to lower Olenekian conodont successions from the Bozhou section, northern Guizhou Province, southwestern China. *Palaeogeography*, *Palaeoclimatology*, *Palaeoecology*, **599**: 111054.

Chen, Y. L., Jiang, H. S., Lai, X. L., Yan, C. B., Richoz, S., Liu, X. D. and Wang, L. N. (2015) Early Triassic conodonts of Jiarong, Nanpanjiang Basin, southern Guizhou Province, South China. *Journal of Asian Earth Science*, **105**: 104–121.

Chen, Y. L., Joachimski, M. M., Richoz, S., Krystyn, L., Aljinović, D., Sirčić, D., Kolar-Jurkovšek, T., Lai, X. and Zhang, Z. (2021) Smithian and Spathian (Early Triassic) conodonts from Oman and Croatia and their depth habitat revealed. Global and Planetary Change, **196**: 103362.

Chen Y. L., Kolar-Jurkovšek, T., Jurkovšek, B., Aljinović. D. and Richoz, S. (2016) Early Triassic conodonts and carbonate carbon isotope record of the Idrija–Žiri area, Slovenia. *Palaeogeography*, *Palaeoclimatology*, *Palaeoecology*, **444**: 84–100.

Chen, Y. L., Richoz, S., Krystyn, L. and Zhang, Z. (2019) Quantitative stratigraphic correlation of Tethyan conodonts across the Smithian-Spathian (Early Triassic) extinction event. *Earth-Sciecne Reviews*, **195**: 37–51.

Dang, T. H. (2006) Mesozoic. In: Thanh, T. D., (Ed.), Stratigraphic Units of Vietnam. Vietnam National University Publishing House, Hanoi, pp. 245–366.

Duan, J. (1987) Permian—Triassic conodonts from southern Jiangsu and adjacent areas, with indexes of their colour alteration. *Acta Micropalaeontologica Sinica*, **4**: 351–368.

Dzik, J. (1976) Remarks on the evolution of Ordovician conodonts. *Acta Palaeontologica Polonica*, **21**: 395–453.

Eichenberg, W. (1930) Conodonten aus dem Culm des Harzes. *Paläontologische Zeitschrift*, **12**: 177–182.

Epstein, A. G., Epstein, J. B. and Harris, L. D. (1977) Conodont color alteration—an idex to organic metamorphism. *United States Geological Survey Professional Paper*, **995**: 1–27.

Galfetti, T., Bucher, H., Martini, R., Hochuli, P. A., Weissert, H., Crasquin-Soleau, S., Brayard, A., Goudemand, N., Brühwiler, T. and Guodun, K. (2008) Evolution of Early Triassic outer platform paleoenvironments in the Nanpanjian Basin (South China) and their significance for the biotic recovery. *Sedimentary Geology*, **204**: 36–60.

Goel, R. J. (1977) Triassic conodonts from Spiti (Himachal Pradesh), India. *Journal of Paleontology*, **51**: 1085–1101.

Goudemand, N., Orchard, M. J., Tafforeu, P., Urdy, S., Brühwiler, T., Brayard, A., Galfetti, T. and Bucher, H. (2012) Early Triassic conodont clusters from South China: Revision of the architecture of the 15 element apparatuses of the superfamily Gondolellidae. *Palaeontology*, **55**: 1021–1034.

Huckriede, R. (1958) Die Conodonten der mediterranen Trias und ihr stratigraphischer Wert. *Paläontologische Ztschrift*, **32**: 141–175.

Hyatt, A. and Smith, J. P. (1905) The Triassic cephalopod genera of America. *United States Geological Survey Professional Paper*, **40**: 1–394.

Igo, H. (2009) Conodonts. In: Shigeta, Y., Zakharov, Y. D., Maeda, H. and Popov, M. A. (Eds.), Lower Triassic System in the Abrek Bay area, South Primorye. National Museum of Nature and Science Monographs 38, Tokyo, pp. 181–196.

Koike, T. (1982) Triassic conodont biostratigraphy in Kedah, West Malaysia. In: Kobayashi, T., Toriyama, R. and Hashimoto, W. (Eds.), Geology and Palaeontology of Southeast Asia 23. University of Tokyo Press, Tokyo, pp. 9–51.

Koike, T. (1988) Lower Triassic conodonts *Platyvillosus* from the Taho Limestone in Japan. *Science Report of the Yokohama National University*, *Section II*, *Biological and*

Geological Sciences, **35**: 61–79.

Koike, T. (1992) Morphological variation in Spathian conodonts *Spathoicriodus collinsoni* (Solien) from the Taho Limestone, Japan. In: Ishizaki, K. and Saito, T. (Eds.), Centenary of Japanese Micropaleontology. Terra Scientific Publishing Company, Tokyo, pp. 355–364.

Komatsu, T. and Dang, T. H. (2007) Lower Triassic bivalve fossils from the Song Da and An Chau Basins, North Vietnam. *Paleontological Research*, **11**: 135–144.

Komatsu, T., Naruse, H., Shigeta, Y., Takashima, R., Maekawa, T., Dang, T. H., Dinh, C. T., Nguyen, D. P., Nguyen, H. H., Tanaka, G. and Sone, M. (2014) Lower Triassic mixed carbonate and siliciclastic setting with Smithian-Spathian anoxic to dysoxic facies, An Chau basin, northeastern Vietnam. *Sedimentary Geology*, **300**: 28–48.

Komatsu, T., Shigeta, Y., Dang, T. H., Nguyen, D. H., Dinh, C. T., Maekawa, T. and Tanaka, G. (2013) *Crittendenia* (Bivalvia) from the Lower Triassic Olenekian Bac Thuy Formation, An Chau Basin, North Vietnam. *Paleontological Research*, **17**: 1–11.

Komatsu, T., Takashima, R., Shigeta, Y., Maekawa, T., Dang, T. H., Dinh, C. T., Sakata, S., Doan, D. H. and Takahashi, O. (2016) Carbon isotopic excursions and detailed ammonoid and conodont biostratigraphy around Smithian-Spathian boundary in the Bac Thuy Formation, Vietnam. *Palaeogeography*, *Palaeoclimatology*, *Palaeoecology*, **454**: 65–74.

Krahl, J., Kauffmann, G., Kozur, H., Richter, D., Foerster, O. and Heinritzi, F. (1983) Neue Daten zur Biostratigraphie und zur tektonischen Lagerung der Phyllit-Gruppe und der Trypali-Gruppe auf der Insel Kreta (Griechenland). *Geologische Rundschau*, **7**: 1147–1166.

Krystyn, L., Brandner, R., Horacek, M. and Richoz, S. (2017) A species of the *Eurygnathodus* costatus morphocline as important auxiliary conodont marker for the *waageni*-date definition of the IOB in low palaeolatitudes. *Geo.Alp*, **14**: 125–126.

Krystyn, L., Richoz, S. and Bhargava, O. N. (2007) The Induan-Olenekian boundary (IOB) in Mud—an update of the candidate GSSP section M04. *Albertiana*, **36**: 33–45.

Li, H., Dong, H., Jiang, H., Wignall, P. B., Chen, Y., Zhang, M., Ouyang, Z., Wu, X., Wu, B., Zhang, Z. and Lai, X. (2022) Integrated conodont biostratigraphy and $\delta^{13}C_{carb}$ records from end Permian to Early Triassic at Yiwagou Section, Gansu Province, northwestern China and their implications. *Palaeogeography*, *Palaeoclimatology*, *Palaeoecology*, **601**: 111079.

Lyu, Z., Orchard, M. J., Chen, Z-Q., Henderson, C. M. and Zhao, L. (2020) A proposed ontogenesis and evolutionary lineage of conodont Eurygnathodus costatus and its role in defining the base of the Olenekian (Lower Triassic). *Palaeogeography*, *Palaeoclimatology*, *Palaeoecology*, **559**: 109916.

Lindström, M. (1970) A suprageneric taxonomy of the conodonts. *Lethaia*, **3**: 427–445.

Maekawa, T. and Igo, H. (2014) Conodonts. In: Shigeta, Y., Komatsu, T., Maekawa, T. and Dang, T. H. (Eds.), Olenekian (Early Triassic) Stratigraphy and Fossil Assemblages in Northeastern Vietnam. National Museum of Nature and Science Monographs 45, Tokyo, pp. 190–271.

Maekawa, T., Komatsu, T. and Koike, T. (2018) Early Triassic conodonts from the Tahogawa Member of the Taho Formation, Ehime Prefecture, Southwest Japan. *Paleontological Research*, supplement to **22**: 1–62.

Maekawa, T., Komatsu, T., Shigeta, Y., Dang, T. H. and Dinh, C. T. (2015) First occurrence of Early Triassic conodonts from the Lang Son Formation, northeastern Vietnam. *Paleontological Research*, **19**: 312–320.

Maekawa, T., Komatsu, T., Shigeta, Y., Dang, T. H., Dinh, C. T. and Nguyen, D. P. (2016) Upper Induan and Lower Olenekian conodont assemblages from the lowest part of the Bac Thuy Formation in the Ban Ru area, northeastern Vietnam. *Proceedings of the 2nd National Scientific Conference of Vietnam Natural Museum System*: 193–207.

Maekawa, T., Komatsu, T., Shigeta, Y., Takashima, R. and Yamaguchi, T. (2021) Carbon isotope chemostratigraphy and conodont biostratigraphy around the Smithian-Spathian boundary in the Panthalassan carbonate succession (SW Japan). *Journal of Asian Earth Sciences*, **205**: 104570.

Matsuda, T. (1984) Early Triassic conodonts from Kashmir, India part 4: *Gondolella* and *Platyvillosus*. *Journal of Geosciences*, *Osaka University*, **27**: 119–141.

Orchard, M. J. (1995) Taxonomy and correlation of Lower Triassic (Spathian) segminate conodonts from Oman and revision of some species of *Neospathodus*. *Journal of Paleontology*, **69**: 110–122.

Orchard, M. J. (2005) Multielement conodont apparatuses of Triassic Gondolelloidea. *Special Papers in Palaeontology*, **73**: 73–101.

Orchard, M. J. (2007) Conodont diversity and evolution through the latest Permian and Early Triassic upheavals. *Palaeogeography*, *Palaeoclimatology*, *Palaeoecology*, **252**: 93–117.

Orchard, M. J. (2010) Triassic conodonts and their role in stage boundary definition. In: Lucas, S. G. (Ed.), The Triassic Timescale. Geological Society of London Special Publications 334, London, pp. 139–161.

Orchard, M. J., and Krystyn, L. (2007) Conodonts from the Induan-Olenekian boundary interval at Mud, Spiti. *Albertiana*, **35**: 30–34.

Perri, M. C., and Andraghetti, M. (1987) Permian-Triassic boundary and Early Triassic conodonts from the southern Alps, Italy. *Rivista Italiana di Paleontologia e Stratigrafia*, **93**: 291–328.

Purnell, M. A., Donoghue, P. C. J. and Aldridge, R. J. (2000) Orientation and anatomical notation in conodonts. *Journal of Paleontology*, **74**: 113–122.

Quenstedt, F. A. (1845–1849) *Petrefactenkunde Deutschlands. Bd. 1. Cephalopoden*. 580 pp., 36 pls. Tübingen.

Shigeta, Y., Zakharov, Y. D., Maeda, H. and Popov, M. A. (2009) *Lower Triassic System in the Abrek Bay area*, *South Primorye*, 218 pp. National Museum of Nature and Science Monographs 38, Tokyo.

Shigeta, Y., Komatsu, T., Maekawa, T. and Dang, T. H., 2014: *Olenekian (Early Triassic) Stratigraphy and Fossil Assemblages in Northeastern Vietnam*, 309 pp. National Museum of Nature and Science Monographs 45, Tokyo.

Solien, M. A. (1979) Conodont biostratigraphy of the Lower Triassic Thaynes Formation, Utah. *Journal of Paleontol-*

ogy, **53**: 276–306.

Staesche, U. (1964) Conodont aus dem Skyth von Südtirol. *Neues Jahr buch für Geologie und Paläontologie*. *Abhandlungen*, **119**: 247–306.

Sweet, W. C. (1970) Uppermost Permian and Lower Triassic conodonts of the Salt Range and Trans-Indus Ranges, West Pakistan. In: Kummel, B. and Teichert, C. (Eds.), Stratigraphic Boundary Problems: Permian and Triassic of West Pakistan. University of Kansas Special Publications 4, Kansas, pp. 207–275.

Sweet, W. C. (1988) *The Conodonta: morphology*, *taxonomy*, *paleoecology*, *and evolutionary history of a long-extinct animal phylum*, 212 pp. Oxford monographs on Geology and Geophysics 10. Clarendon Press, Oxford.

Takahashi, O., Maekawa, T., Dumitrica, P., Nguyen, D. P., Komatsu, T. (2022) Latentifistularia and other radiolarian species from the lower Smithian (Lower Triassic) Lang Son Formation, NE Vietnam. *Revue de micropaléontologie*, **75**: 100610.

Takahashi, O., Maekawa, T., Komatsu, T., Nguyen, D. P., Dinh, C. T. and Doan, D. H. (2017) Early Spathian (Late Olenekian, Early Triassic) radiolaria from the Bac Thuy Formation, northeastern Vietnam. *Revue de micropaléontologie*, **60**: 171–178.

Tian, C., Dai, J. and Tian, S. (1983) Triassic conodonts. In: Chenghu Institute of Geology and Mineral Resources (Ed.), Paleontological Atlas of Southwest China, Volume of Microfossils. Geological Publishing House, Beijing, pp. 345–398. (in Chinese)

Vu Khuc (1984) *Triassic Ammonoids in Vietnam*. 134 pp. Geoinform and Geodate Institute, Hanoi. (in Vietnamese with English abstract)

Vu Khuc (1991) Paleontological Atlas of Vietnam, Vol. 3, Mollusca. 207 pp. Science and Technics Publishing House, Hanoi.

Wang, Z. and Cao, Y. (1981) Early Triassic conodonts from the Jiangyou-beichuan area, Sichuan, Western Hubei. *Acta Palaeontologica*, *Sinica*, **20**: 363–375. (in Chinese with English abstract)

Wang, Z. and Zhong, D. (1994) Triassic conodonts from different facies in eastern Yunnan, western Guizhou and northern Guangxi. *Acta Micropalaeontologica Sinica*, **11**: 379–412.

Zhao, L. S., Orchard, M. J., Tong, J. N., Sun, Z. M., Zuo, J. X., Zhang, S. I. and Yun, A. L. (2007) Lower Triassic conodont sequence in Chaohu, Anhui Province, China and its global correlation. *Palaeogeography*, *Palaeoclimatology*, *Palaeoecology*, **252**: 24–38.

Appendix. Lists of some specimens of the genus *Icriospathodus*. Parenthesis shows measurement of broken specimen. "+" shows the number of preserved denticles on incomplete specimens. "?" indicates inferred parts.

Number	Species	Nation	Locality	Information of specimens Figure no.	Reference	Geologic time scale	Element Length (mm)	Element Width (mm)	L/W	Denticle no.	Denticles on the basal cup	Form of basal cavity	Remarks
Iz1	*Icriospathodus zaksi*	Russia	—	Taf. XVIII.3	Buryi, 1979	—	0.54	0.14	3.9	8+	a side	Asymmetrical oval?	Holotype
Iz2	*Icriospathodus zaksi*	Italy	CG 5	Pl. 33.1	Perri & Andraghetti, 1987	lower Spathian?	0.67	0.16	4.2	11	—	Subtriangular	Identified as *Ns. triangularis*
Iz3	*Icriospathodus zaksi*	Italy	CG 5	Pl. 33.2	Perri & Andraghetti, 1987	lower Spathian?	0.79	0.16	4.9	11	—	Subtriangular	Identified as *Ns. triangularis*
Iz4	*Icriospathodus zaksi*	Italy	CG 5	Pl. 33.3	Perri & Andraghetti, 1987	lower Spathian?	0.61	—	—	14+	—	—	Identified as *Ns. triangularis*
Iz5	*Icriospathodus zaksi*	Italy	CG 5	Pl. 33.4	Perri & Andraghetti, 1987	lower Spathian?	0.58	0.12	4.8	14+	—	Subtriangular	Identified as *Ns. triangularis*
Iz6	*Icriospathodus zaksi*	Slovenia	61/3	Fig. 8.10	Chen *et al.*, 2016	lower Spathian	0.31	0.08	3.9	7?	—	Asymmetrical oval	Identified as *Ns. robusuts*
Iz7	*Icriospathodus zaksi*	Slovenia	61/6	Fig. 8.8	Chen *et al.*, 2016	lower Spathian	0.26	0.05	5.2	11?	—	Subrounded	Identified as *Ns. robusuts*
Iz8	*Icriospathodus zaksi*	Oman	WBK08/8	Fig. 6.4	Chen *et al.*, 2019	uppermost Smithian	0.53	0.11	4.8	13+	both side	Subrounded	
Iz9	*Icriospathodus zaksi*	Oman	WBK08/8	Fig. 7.9	Chen *et al.*, 2019	uppermost Smithian	0.43	0.09	4.8	9	both side	Subrounded	
Iz10	*Icriospathodus zaksi*	Oman	WBK08/8	Fig. 7.10	Chen *et al.*, 2019	uppermost Smithian	0.42	0.10	4.2	8	both side	Asymmetrical oval	Figs. 6.11, 6.12 of Chen *et al.*, 2021
Iz11	*Icriospathodus zaksi*	Oman	RT25C	Fig. 3.13	Chen *et al.*, 2019	lower Spathian	0.66	0.12	5.5	12	—	Subtriangular	Identified as *Ic. crassatus*
Iz12	*Icriospathodus zaksi*	Oman	WBK08/8	Fig. 3.11	Chen *et al.*, 2021	uppermost Smithian	0.44	0.12	3.7	9+	—	Oval?	Identified as *Ic. crassatus*
Iz13	*Icriospathodus zaksi*	Oman	RT28	Fig. 6.10	Chen *et al.*, 2021	lower Spathian	0.71	0.16	4.4	15	—	Rectangular	Identified as *Ic. crassatus*
Iz14	*Icriospathodus zaksi*	Vietnam	KC02-10	Figs. 192.14–192.17	Maekawa & Igo, 2014	uppermost Smithian	0.65	0.18	3.6	6+	both side	Subrounded	
Iz15	*Icriospathodus zaksi*	Vietnam	KC02-10	Figs. 192.18–192.21	Maekawa & Igo, 2014	uppermost Smithian	0.60	0.21	2.9	12	—	Asymmetrical oval	
Iz16	*Icriospathodus zaksi*	Vietnam	NT01-07	Figs. 192.22–192.25	Maekawa & Igo, 2014	uppermost Smithian	0.49	0.14	3.5	9	—	Rectangular	
Iz17	*Icriospathodus zaksi*	Vietnam	NT01-09	Figs. 192.26–192.29	Maekawa & Igo, 2014	uppermost Smithian	(0.31)	0.08	—	7+	—	Asymmetrical oval	broken
Iz18	*Icriospathodus zaksi*	Vietnam	BR01-02	Fig. 5C	this study	uppermost Smithian	0.42	0.09	4.7	7	—	Drop	
Iz19	*Icriospathodus zaksi*	Vietnam	BR01-02	Fig. 5D	this study	uppermost Smithian	(0.42)	0.09	—	6+	—	—	
Iz20	*Icriospathodus zaksi*	Vietnam	BR01-02	Fig. 5E	this study	uppermost Smithian	0.46	0.16	2.9	8	—	Asymmetrical oval	
Iz21	*Icriospathodus zaksi*	Vietnam	BR01-02	Fig. 5F	this study	uppermost Smithian	0.53	0.11	4.8	9	—	Elliptical	
Iz22	*Icriospathodus zaksi*	Vietnam	BR01-02	Fig. 5G	this study	uppermost Smithian	0.44	0.12	3.7	9	—	Oval	
Iz23	*Icriospathodus zaksi*	Japan	W01-49	Fig. 29.20	Maekawa *et al.*, 2018	lower Spathian	0.79	0.25	3.2	11	—	Subrounded	
Iz24	*Icriospathodus zaksi*	Japan	E01-19	Fig. 29.21	Maekawa *et al.*, 2018	lower Spathian	0.51	0.17	3.0	9+	—	Subrounded	broken
Iz25	*Icriospathodus zaksi*	Japan	E03-09	Fig. 29.22	Maekawa *et al.*, 2018	lower Spathian	0.61	0.15	4.1	11	—	Subtriangular	
Iz26	*Icriospathodus zaksi*	Japan	E03-09	Fig. 29.23	Maekawa *et al.*, 2018	lower Spathian	0.60	0.11	5.5	9?	—	Subrounded	
Iz27	*Icriospathodus zaksi*	Japan	E03-09	Fig. 29.24	Maekawa *et al.*, 2018	lower Spathian	0.53	0.11	4.8	9	—	Subrounded	
Iz28	*Icriospathodus zaksi*	Japan	E03-09	Fig. 29.25	Maekawa *et al.*, 2018	lower Spathian	0.37	0.08	4.6	8	—	Subrounded	
Iz29	*Icriospathodus zaksi*	Japan	E01-11	Fig. 29.26	Maekawa *et al.*, 2018	lower Spathian	0.65	0.15	4.3	12	—	Asymmetrical oval	
Ic1	*Icriospathodus crassatus*	Italy	CG 5	Pl. 33.5	Perri & Andraghetti, 1987	lower Spathian?	0.67	0.07	9.6	15	—	Asymmetrical oval	Identified as *Ns. triangularis*
Ic2	*Icriospathodus crassatus*	Oman	GSC C-177654	Figs. 2.19, 2.25, 2.27	Orchard, 1995	lower Spathian	0.58	0.07	8.3	13	—	Subtriangular	Holotype
Ic3	*Icriospathodus crassatus*	Oman	RT28	Fig. 5.5	Chen *et al.*, 2019	lower Spathian	0.66	0.10	6.6	15	—	Subrounded	Identified as *Tr. symmetricus*
Ic4	*Icriospathodus crassatus*	Oman	RT28	Fig. 6.1	Chen *et al.*, 2019	lower Spathian	0.69	0.08	8.6	18?	—	Subrounded	
Ic5	*Icriospathodus crassatus*	Oman	WBK05/15	Fig. 6.7	Chen *et al.*, 2019	lower Spathian	0.45	0.07	6.4	12	—	Subtriangular	
Ic6	*Icriospathodus crassatus*	Oman	WBK11	Fig. 3.12	Chen *et al.*, 2021	lower Spathian	0.45	0.07	6.4	14+		Asymmetrical oval	
Ic7	*Icriospathodus crassatus*	Oman	WBK11	Fig. 3.13	Chen *et al.*, 2021	lower Spathian	0.53	0.06	8.8	18	posterior margin	Asymmetrical oval	
Ic8	*Icriospathodus crassatus*	Oman	WBK11	Fig. 3.14	Chen *et al.*, 2021	lower Spathian	0.70	0.16	4.4	18+	a side	Parallelogram	
Ic9	*Icriospathodus crassatus*	Oman	WBK11	Fig. 3.15	Chen *et al.*, 2021	lower Spathian	0.59	0.10	5.9	16?	a side	Parallelogram	
Ic10	*Icriospathodus crassatus*	Oman	WBK11	Fig. 4.1	Chen *et al.*, 2021	lower Spathian	0.53	0.11	4.8	16	—	Subrounded	
Ic11	*Icriospathodus crassatus*	Oman	WBK11	Fig. 4.2	Chen *et al.*, 2021	lower Spathian	0.54	0.11	4.9	14	—	Subtriangular	
Ic12	*Icriospathodus crassatus*	Oman	WBK12	Fig. 4.12	Chen *et al.*, 2021	lower Spathian	(0.47)	0.09	—	10+	posterior margin	Parallelogram	broken
Ic13	*Icriospathodus crassatus*	Oman	WBK12	Fig. 4.13	Chen *et al.*, 2021	lower Spathian	0.56	0.09	6.2	17	a side	Parallelogram	Identified as *Ic. zaksi*
Ic14	*Icriospathodus crassatus*	Oman	WBK12	Fig. 4.14	Chen *et al.*, 2021	lower Spathian	0.85	0.10	8.5	15	—	Parallelogram	Identified as *Tr. homeri*
Ic15	*Icriospathodus crassatus*	Vietnam	KC02-15	Figs. 192.7–192.9	Maekawa & Igo, 2014	lower Spathian	0.52	0.11	4.7	11	—	Subsquare	
Ic16	*Icriospathodus crassatus*	Japan	1119	Figs. 12.9, 12.10	Koike, 1992	lower Spathian	0.52	0.09	5.8	11	posterior margin	Asymmetrical oval	
Ic17	*Icriospathodus crassatus*	Japan	9	Fig. 12.52	Koike, 1992	lower Spathian	(0.50)	0.12	—	9+	both side	Parallelogram	broken
Ic18	*Icriospathodus crassatus*	Japan	9	Fig. 13.3	Koike, 1992	lower Spathian	0.67	0.12	5.6	—	a side	Asymmetrical oval	broken
Ic19	*Icriospathodus crassatus*	Japan	9	Fig. 13.5	Koike, 1992	lower Spathian	0.82	0.17	4.8	15	both side	Asymmetrical oval	broken
Ic20	*Icriospathodus crassatus*	Japan	9	Figs. 13.6, 13.7	Koike, 1992	lower Spathian	0.84	0.20	4.2	16+	both side	Subtriangular	

Appendix. Continued.

Number	Species	Nation	Locality	Information of specimens Figure no.	Reference	Geologic time scale	Element		L/W	Denticle no.	Denticles on the basal cup	Form of basal cavity	Remarks
							Length (mm)	Width (mm)					
Ic21	*Icriospathodus crassatus*	Japan	W01-49	Fig. 29.8	Maekawa *et al.*, 2018	lower Spathian	(0.42)	0.07	—	8 +	—	Drop	
Ic22	*Icriospathodus crassatus*	Japan	W01-50	Fig. 29.9	Maekawa *et al.*, 2018	lower Spathian	(0.47)	0.08	—	10 +	—	Subrounded	broken
Ic23	*Icriospathodus crassatus*	Japan	W01-50	Fig. 29.10	Maekawa *et al.*, 2018	lower Spathian	0.48	0.10	4.8	9	—	Subtriangular	
Ic24	*Icriospathodus crassatus*	Japan	E02-11	Fig. 29.11	Maekawa *et al.*, 2018	lower Spathian	0.49	0.10	4.9	11	—	Subrounded	
Ic25	*Icriospathodus crassatus*	Japan	E03-09	Fig. 29.12	Maekawa *et al.*, 2018	lower Spathian	0.43	0.08	5.4	8	—	Subrounded	
Ic26	*Icriospathodus crassatus*	Japan	E03-09	Fig. 29.13	Maekawa *et al.*, 2018	lower Spathian	0.61	0.11	5.5	12	—	Subtriangular	
Ic27	*Icriospathodus crassatus*	Japan	E03-09	Fig. 29.14	Maekawa *et al.*, 2018	lower Spathian	0.61	0.08	7.6	12	—	Subrounded	
Ic28	*Icriospathodus crassatus*	Japan	E03-09	Fig. 29.15	Maekawa *et al.*, 2018	lower Spathian	0.63	0.11	5.7	11 +	—	Subrounded	
Ic29	*Icriospathodus crassatus*	Japan	E03-09	Fig. 29.16	Maekawa *et al.*, 2018	lower Spathian	0.41	0.07	5.9	10	—	Drop	
Ic30	*Icriospathodus crassatus*	Japan	E03-10	Fig. 29.17	Maekawa *et al.*, 2018	lower Spathian	(0.50)	0.10	—	11 +	—	Subtriangular	broken
Ic31	*Icriospathodus crassatus*	Japan	E03-11	Fig. 29.18	Maekawa *et al.*, 2018	lower Spathian	0.63	0.08	7.9	13 +	—	Asymmetrical oval	
Ic32	*Icriospathodus crassatus*	Japan	E03-11	Fig. 29.19	Maekawa *et al.*, 2018	lower Spathian	0.76	0.13	5.8	13	—	Subtriangular	
	Icriospathodus collinosni	Oman	WBK12	Fig. 4.9	Chen *et al.*, 2021	lower Spathian	0.87	0.25	3.5	20	both side	Parallelogram	
	Icriospathodus collinosni	Oman	WBK12	Fig. 4.10	Chen *et al.*, 2021	lower Spathian	0.95	0.26	3.7	17	posterior margin	Parallelogram	
	Icriospathodus collinosni	Oman	WBK12	Fig. 4.11	Chen *et al.*, 2021	lower Spathian	0.57	0.19	3.0	13	posterior margin	Parallelogram	
	Icriospathodus collinosni	Japan	9	Fig. 13.25	Koike, 1992	lower Spathian	0.77	0.17	4.5	12	posterior margin	Parallelogram	
	Icriospathodus collinosni	Japan	9	Fig. 13.26	Koike, 1992	lower Spathian	(0.88)	0.21	—	11 +	a side	Parallelogram	broken
	Icriospathodus collinosni	Japan	9	Fig. 13.29	Koike, 1992	lower Spathian	0.88	0.22	4.0	13	a side	Parallelogram	
	Icriospathodus collinosni	Vietnam	KC02-14	Figs. 186.10–186.13	Maekawa & Igo, 2014	lower Spathian	0.69	0.14	4.9	14	posterior margin	Parallelogram	
	Icriospathodus collinosni	Vietnam	KC02-15	Figs. 191.1–191.3	Maekawa & Igo, 2014	lower Spathian	0.81	0.17	4.8	15	a side	Parallelogram	
	Icriospathodus collinosni	Vietnam	KC02-15	Figs. 192.4–192.5	Maekawa & Igo, 2014	lower Spathian	(0.47)	0.27	—	8 +	a side	Parallelogram	broken